DEBRIS ATTITUDE MOTION MEASUREMENTS AND MODELING – OBSERVATION VS. SIMULATION

T. Lips[(1)], R. Kanzler[(1)], A. Breslau[(1)], P. Kärräng[(1)], J. Šilha[(2)], T. Schildknecht[(2)], D. Kucharski[(3)], G. Kirchner[(4)], J. Rosebrock[(5)], D. Cerutti-Maori[(5)], and H. Krag[(6)]

[(1)]*HTG – Hypersonic Technology Göttingen GmbH, Germany, Email: t.lips@htg-hst.de*
[(2)]*AIUB – Astronomical Institute of the University of Bern, Switzerland*
[(3)]*SERC – Space Environment Research Centre, Canberra, Australia*
[(4)]*IWF – Space Research Institute of the Austrian Academy of Sciences, Graz, Austria*
[(5)]*FHR – Fraunhofer Institute for High Frequency Physics and Radar Techniques, Wachtberg, Germany*
[(6)]*ESA – European Space Agency, Darmstadt, Germany*

ABSTRACT

End of 2014, ESA initiated a research project named “Debris Attitude Motion Measurements and Modeling”. The main goal of this project was to combine space debris attitude state information, obtained by different means of observation, with numerical simulations. Under the lead of AIUB, light curves and laser ranging residuals were obtained by AIUB and IWF, while FHR conducted radar observations. In parallel, HTG developed a 6 degrees-of-freedom – orbit and attitude – propagator. This tool called ιOTA (In-Orbit Tumbling Analysis) takes into account all relevant external and internal perturbation sources (gravity, aerodynamics, solar radiation pressure, electromagnetic, etc.).

The final phase of the project was a critical comparison between observation data obtained for various space objects (e.g. ENVISAT, LAGEOS-2) and the corresponding simulation results. This comparison also served the purpose of software validation for ιOTA.

The conversion of observation data into well-defined attitude states (i.e. rotation vector orientation and magnitude) can be quite difficult and sometimes resulting into multiple, non-unique solutions. Therefore, this comparison used an inverse approach. ιOTA is capable to convert its propagation results into synthetic observation results. This conversion takes into account the individual sensor type and relative perspective towards the observation target during the measurement campaign. This approach facilitates a direct comparison of real observation data (light curves, laser ranging residuals, and radar imaging) with the numerical propagation results.

This paper presents the attitude propagation methods of ιOTA and the results of its software validation process showing a comparison between real and synthetic observation data.

NOMENCLATURE

$\vec{B}$	Magnetic field
t	Time
λ	Damping coefficient
$\vec{\omega}$	Angular velocity

1. INTRODUCTION

Today, there is little knowledge on the attitude state of decommissioned intact objects in Earth orbit. Observational means have advanced in the past years, but are still limited with respect to an accurate estimate of motion vector orientations and magnitude. Especially for the preparation of Active Debris Removal (ADR) missions as planned by ESA’s Clean Space initiative or contingency scenarios for ESA spacecraft like ENVISAT, such knowledge is needed.

ESA’s “Debris Attitude Motion Measurements and Modelling” project (ESA Contract No. 4000112447/14/D/SR), led by the Astronomical Institute of the University of Bern (AIUB), addressed this problem. The goal of the project was to achieve a good understanding of the attitude evolution and the considerable internal and external effects which occur. To characterize the attitude state of selected targets in LEO and GTO, multiple observation methods have been combined. Optical observations were carried out by AIUB, Satellite Laser Ranging (SLR) was performed by AIUB and the Space Research Institute of the Austrian Academy of Sciences (IWF) and radar measurements and signal level determination are provided by the Fraunhofer Institute for High Frequency Physics and Radar Techniques (FHR).

2. ιOTA

The In-Orbit Tumbling Analysis tool (ιOTA) is a prototype software, developed by Hypersonic Technology Göttingen GmbH (HTG) within the framework of this project. ιOTA is a highly modular software tool to perform short- (days), medium- (months) and long-term (years) propagation of the orbit and attitude motion (six degrees-of-freedom) of spacecraft in Earth orbit. The simulation takes into account all relevant acting forces and torques, including aerodynamic drag, solar radiation pressure, gravitational influences of Earth, Sun and Moon, eddy current damping, impulse and momentum transfer from space debris or micro-meteoroid impact, as well as the optional definition of particular spacecraft specific influences like tank sloshing, reaction wheel behavior, magnetic torquer activity and thruster firing.

The purpose of ιOTA is to provide high accuracy short-term simulations to support observers and potential active debris removal missions, as well as medium- and long-term simulations to study the significance of the particular internal and external influences on the attitude, especially damping factors and momentum transfer. The simulation also enables the investigation of the altitude dependency of the particular external influences. ιOTA's post-processing modules can generate synthetic measurements for observers and for software validation. The validation of the software has been done by cross-calibration with observations and measurements acquired by the project partners.

For the attitude simulation, the user has to provide spacecraft specific mandatory input that is needed regardless of which simulation modules have been selected in particular. Additional input is needed, if the user chooses to include AOCS (Attitude and Orbit Control System) activation, tank sloshing, specific impact or leakage events into the simulation.

Mandatory input for the simulation is the initial spacecraft orbit and attitude, as well as the corresponding epoch. Also a panel based surface geometry model of the spacecraft (as shown in Fig. 1 for the Delta-II second stage) has to be provided by the user. The spacecraft mass, moments of inertia (MOI) and the center of mass (CoM) position within the surface geometry model have to be defined by the user.

The environmental conditions for the attitude simulation comprise the modeling of forces and torques resulting from atmospheric drag, gravitational influences from Earth, Sun and Moon, eddy current damping caused by the tumbling motion inside the Earth's magnetosphere, solar radiation pressure and impulse transfer through micro-meteoroid and small space debris impact.

To simulate the influence of atmospheric drag, the aerodynamic force and torque coefficients are calculated for the stream facing side of the spacecraft using the spacecraft surface geometry model and including shadowing effects resulting from the objects actual attitude. The standard atmosphere model used by ιOTA is NRLMSISE-00 [3].

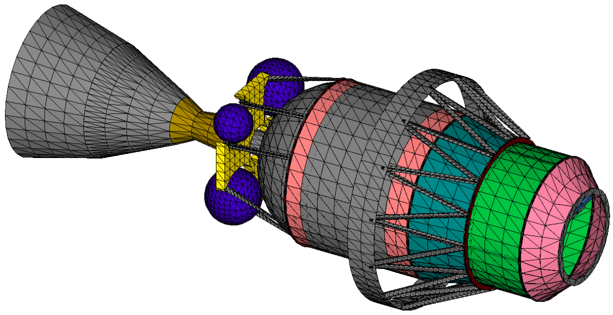

Figure 1. Panel based geometry model of Delta-II second stage

The calculation of gravitational effects is done separately for the acceleration and torques caused by Earth and the third-body accelerations caused by the Sun and Moon. The geoid models implemented and supported by ιOTA are EGM96 [4] and EGM2008 [5], both up to order and degree 42. To determine the gravitational acceleration caused by Sun and Moon, the solar and lunar positions are calculated using approximations according to Vallado [6]. The accuracy of the calculated third-body positions has been verified using high-precision ephemeris from NASA's HORIZONS Web-Interface [7].

One of the essential effects on satellites in Earth orbit and particularly relevant for ADR missions is eddy current damping. The properties of the Earth magnetic field needed for the simulation are provided by the latest World Magnetic Model WMM2015 [8]. For eddy current damping, exponential decay is assumed, based on:

$$\vec{\omega}(t) = \vec{\omega}_0 \cdot \mathrm{e}^{-\lambda \cdot t} \tag{1}$$

The damping coefficient λ has to be determined from observations. It has to be calibrated with an additional calibration factor, which accounts for spacecraft related and in general unknown parameters, like surface conductivity. The general assumption for eddy current damping calculation in ιOTA is, that these spacecraft specific parameters are either unknown or have high uncertainties. Thus, they are replaced by one calibration factor.

The damping method implemented also considers the current position and attitude motion of the object within the Earth's magnetic field and the local magnetic field vector, to determine the effective direction and magnitude of the damping through:

$$\vec{B} \times (\vec{\omega} \times \vec{B}) \tag{2}$$

Due to the potentially complex electromagnetic properties of spacecraft and the general purpose of ιOTA to be used for a wide range of decommissioned objects, an implementation of a more sophisticated eddy current damping calculation, e.g. like done by Praly [9] or Ortiz Gómez and Walker [10], was discarded.

The acting acceleration and torques resulting from solar radiation pressure are calculated using the solar constant at 1 AU. For the actual attitude of the spacecraft the illuminated surface parts as well as the angle of incidence for each surface geometry panel are determined based on the solar position and the surface geometry model, including shadowing effects by Earth and the spacecraft geometry itself.

As a reference, the resulting angular accelerations by gravitational, aerodynamic and solar radiation pressure acting on a Delta-II second stage in a low earth orbit (LEO) have been compared with the SCARAB (Spacecraft Atmospheric Re-entry and Aerothermal Break-up) software [11]. The corresponding results are plotted in Figs. 2 and 3 as function of the flight altitude for several orbits.

The gravitational angular acceleration is due to the gravity gradient of Earth's gravity field. Its maximum value (for maximum out-of-equilibrium attitude) scales with the distance to the Earth center, and is therefore quite insensitive to altitute variations in LEO. Its minimum values are zero for the equilibrium attitudes. The solar radiation induced angular acceleration scales with the distance to the Sun and is therefore even less sensitive to the flight altitude than the gravitational angular acceleration. In detail it depends on the spacecraft attitude relative to the sunlight and on the optical properties of the surface. It is zero if the spacecraft is in the Earth shadow. The aerodynamic angular acceleration scales with the atmospheric density, which is a function of the altitude above the Earth surface. Therefore, the aerodynamic angular acceleration varies strongly with the flight altitude. In detail it depends on the attitude relative to the flight direction and on the material properties of the surface.

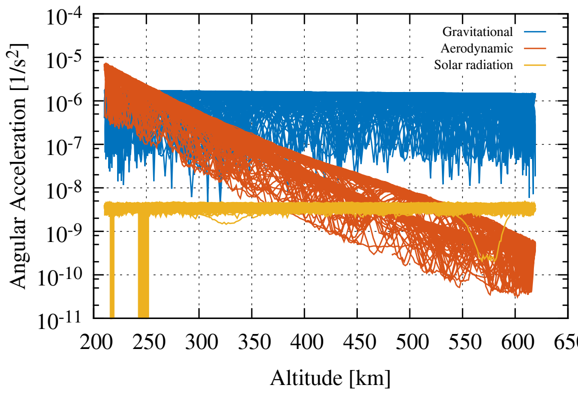

Figure 2. Altitude dependent angular acceleration of the Delta-II second stage (SCARAB)

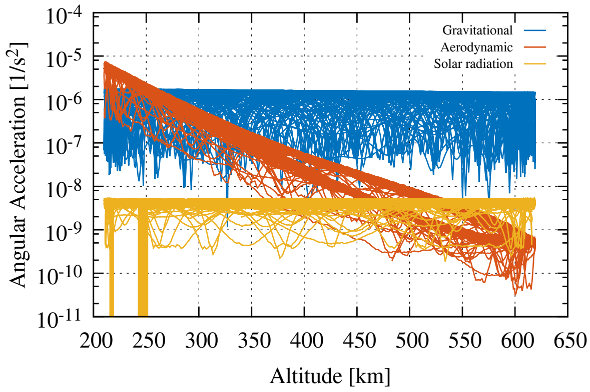

Figure 3. Altitude dependent angular acceleration of the Delta-II second stage (ιOTA)

3. ENVISAT

The primary test object for ιOTA validation was ENVISAT. ENVISAT is a European Earth observation mission launched in 2002. The mission ended on April 8, 2012, following the unexpected loss of contact with the satellite. Due to the rather high risk for ENVISAT to be involved in a catastrophic collision with space debris, ESA is considering to conduct an active debris removal mission. For such a mission, including a docking maneuver to an uncooperative target, accurate knowledge and reliable prediction of the attitude state is essential.

Fig. 4 shows the geometry model of ENVISAT used by ιOTA. The following mass related properties have been used:

- Mass: 7827.867 kg
- Center of mass: -3.905, -0.009, 0.003 m
- Moments of inertia: 17023.3, 124825.7, 129112.2, 397.1, -2171.1, 344.2 kg/m^2

The reflectivity properties of the satellite, a diffuse factor, for light curve generation have been set 0.7. This means that 70% of the sun light is reflected diffusely and 30% specular.

4. ENVISAT OBSERVATION CAMPAIGN

During a collaborative measurements night on September 21, 2016, two passages (Fig. 13) of the ENVISAT satellite above Europe have been observed by AIUB (Fig. 5), IWF (Fig. 6), and FHR (Fig. 7). Light curves for both passages (Figs. 8 and 9) and SLR residuals for the second passage (Fig. 10) have been obtained by AIUB. Radar images for both passages (Figs. 11 and 12) have been

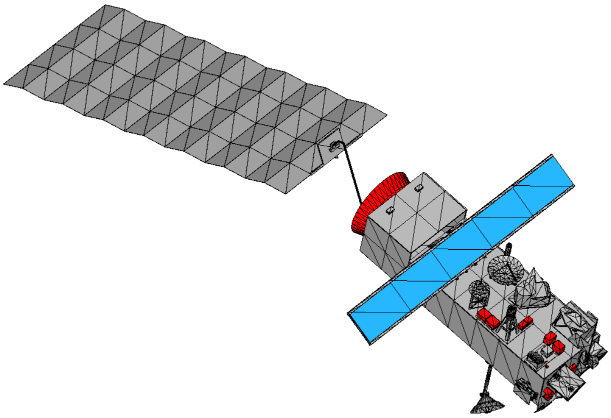

Figure 4. ENVISAT ιOTAmodel

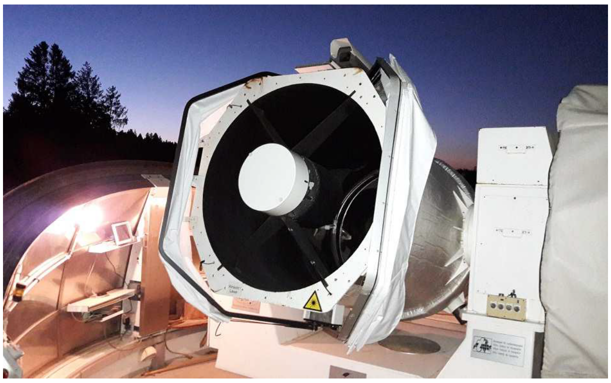

Figure 5. ZIMLAT telescope at AIUB, Switzerland

obtained by FHR. IWF observations were blocked by clouds, unfortunately.

Tab. 1 shows three attitude states derived from the measurement campaign. All states show that the main rotation is about the body-fixed z-axis (yaw motion), as illustrated in Fig. 14. However, the ISAR-derived states (IDs 1.0 and 2.0) indicate a change in rotation vector between the first and the second passage. The SLR-derived state (ID 3.0) indicates a perfect yaw rotation because SLR measurements allows only the determination of the rotation period.

In the next section, the ιOTA software will be used for numerical rebuilding of the two ENVISAT passages in order to resolve these attitude state discrepancies.

Figure 6. SLR station Graz of IWF, Austria

5. ENVISAT NUMERICAL PASSAGE REBUILDING

ιOTA has been used to numerically rebuild the two observed ENVISAT passages and to generate synthetic measurement results (light curves, SLR residuals, and ISAR images) which could be compared directly with the real measurement data. By iteratively adapting the used initial attitude state (see Tab.2), an optimized solution could be found which fits best with the measurements and closes as well the gap between the two passages.

Figs. 15 and 16 show a comparison between observed and simulated light curves for the two passages. These plots reveal that the light curves simulated with ιOTA are not correct, at least for a complex shape like ENVISAT. This is caused by the simplification of using just one unique light reflection parameter for the whole surface of the spacecraft.

Fig. 17 shows an excellent agreement between observed and simulated SLR residuals for the second passage. ιOTA simulations also revealed why no SLR data could be recorded during the first passage: the laser retroreflector was not visible for ZIMLAT. This was also con-

Figure 7. Tracking and Imaging Radar (TIRA) of FHR, Germany

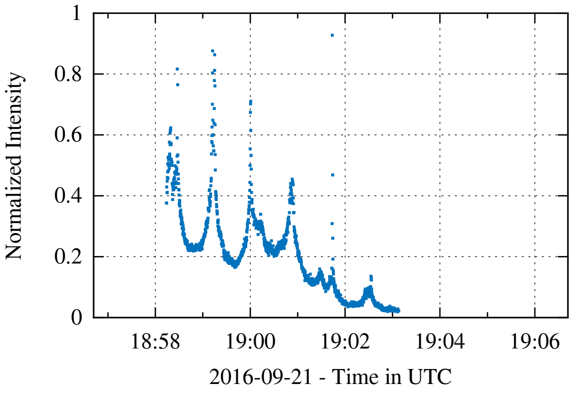

Figure 8. ENVISAT light curve, first passage

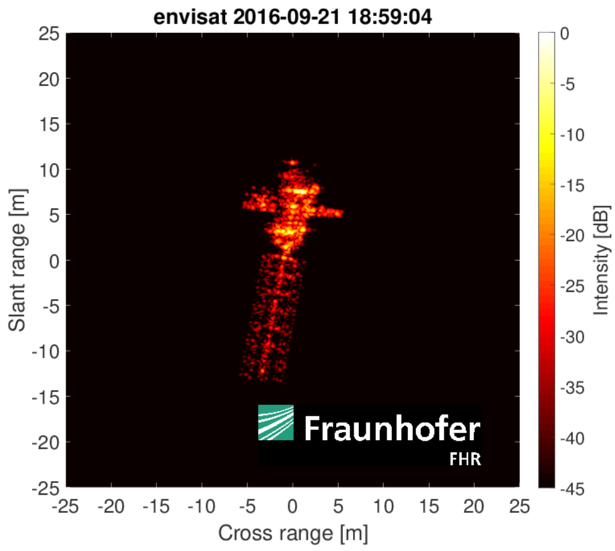

Figure 11. ENVISAT ISAR image, first passage

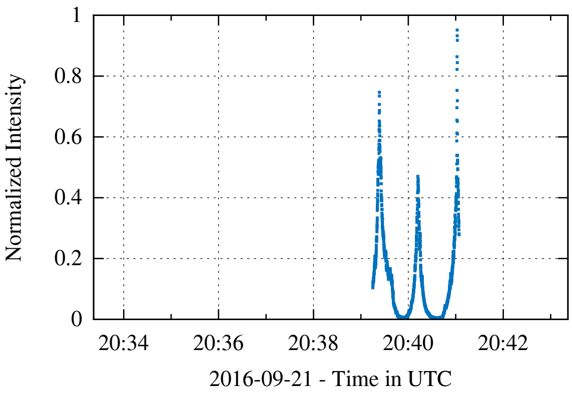

Figure 9. ENVISAT light curve, second passage

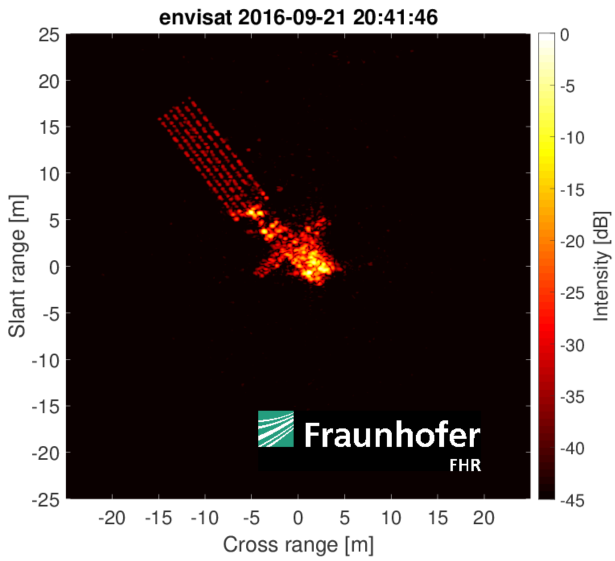

Figure 12. ENVISAT ISAR image, second passage

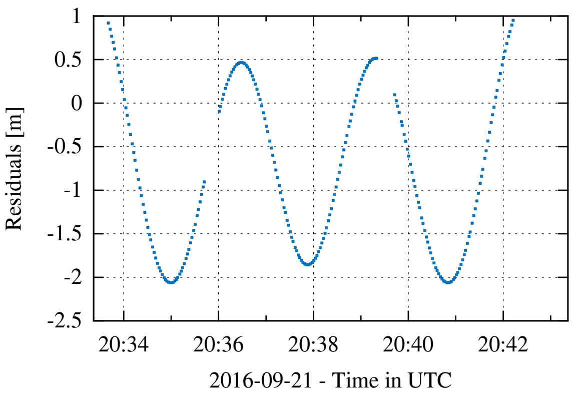

Figure 10. ENVISAT SLR residuals, second passage

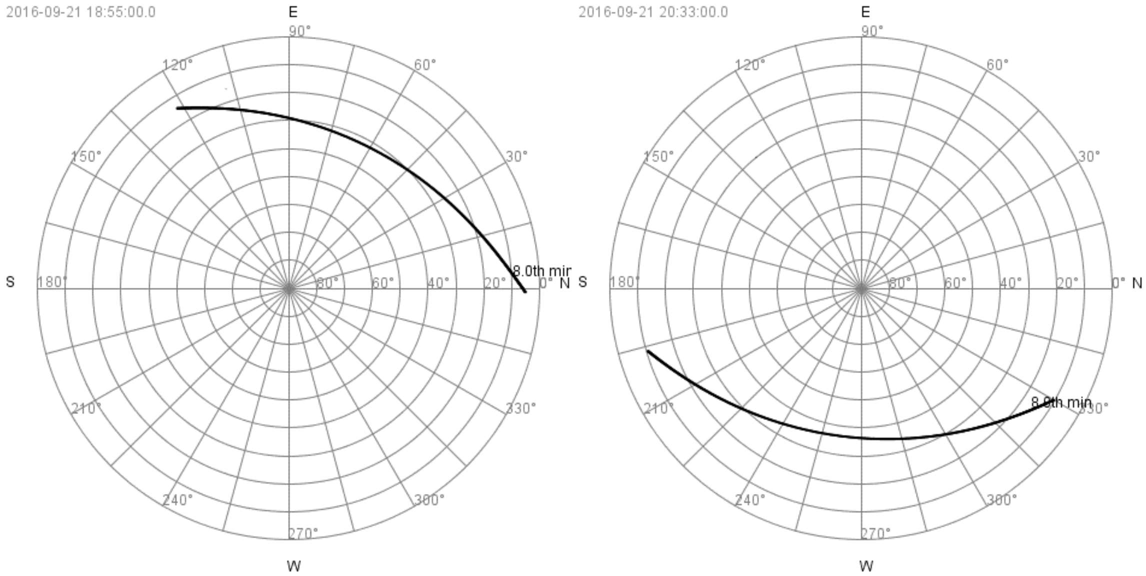

Figure 13. ENVISAT passages over ZIMLAT

Table 1. ENVISAT attitude states derived from observations

State ID	Time (UTC)	Source	Attitude angles [deg] (roll, pitch, yaw angle)	Angular velocities [deg/s] (roll, pitch, yaw rate)
1.0	18:53:21.9	ISAR	151.2, -58.3, -102.1	-0.704, -0.135, -1.486
2.0	20:32:22.9	ISAR	95.6, 69.6, -31.4	-0.096, -0.110, -1.6377
3.0	20:31:18.6	SLR	117.0, -46.3, -69.8	0.0, 0.0, -1.6774

Table 2. ENVISAT attitude states derived with ιOTA

State ID	Time (UTC)	Source	Attitude angles [deg] (roll, pitch, yaw angle)	Angular velocities [deg/s] (roll, pitch, yaw rate)
1.1	18:53:21.9	ιOTA	147.0, -76.0, -102.0	0.04, 0.025, -1.659
2.1	20:32:22.9	ιOTA	116.8, 53.3, -23.7	0.11, -0.069, -1.655
3.1	20:31:18.9	ιOTA	108.1, -48.8, -58.0	0.06, 0.020, -1.659

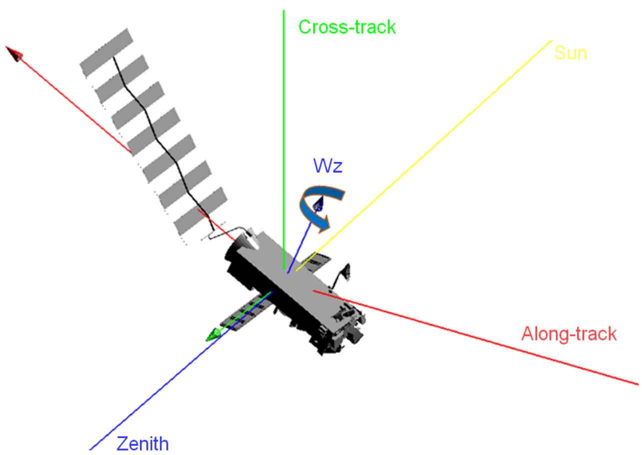

Figure 14. ENVISAT main rotation axis

firmed by the results of FHR.

Figs. 18 through 21 show an almost perfect match between simulated ISAR images and the images recorded by FHR. The figures produced by ιOTA include also depictions of the apparent optical view/orientation towards the observer in order to facilitate the interpretation of the simulated radar images.

The full evolution of the individual attitude rates from the first passage to the second is depicted in Fig. 22. The yaw rate is almost undisturbed at -1.648 ± 0.014 deg/s, while the roll and pitch rates show clear oscillations with a period of 451 secs – roll rate: 0.032 ± 0.082 deg/s; pitch rate: -0.127 ± 0.154 deg/s. The total mean tumbling rate of ENVISAT during these two passages was 1.66 deg/s.

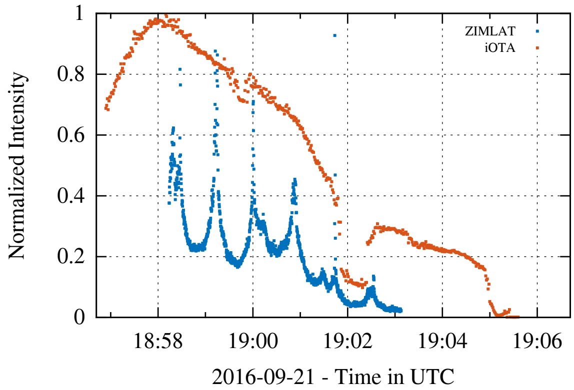

Figure 15. ENVISAT simulated light curve, first passage

6. ENVISAT LONG-TERM SIMULATION

Long-term attitude motion simulation of ENVISAT have been conducted to validate the ιOTA prediction modules. The evolution of the inertial angular velocity over time has been monitored. The following parameters have been used as input:

- Initial epoch: 2013-07-13, 21:43:12.0 (UTC)
- Initial attitude state: determined from SLR by AIUB
  - Euler angles (roll, pitch, yaw): 0 deg, 0 deg, -78.499 deg
  - Rotation vector (roll, pitch, yaw rate): 0 deg/s, 0 deg/s, -2.735 deg/s
- Initial orbit state: generated by using TLE and SGP4 model
- Model: ENVISAT 3D model based on refined SCARAB model
- Simulation time: approx. 400 days

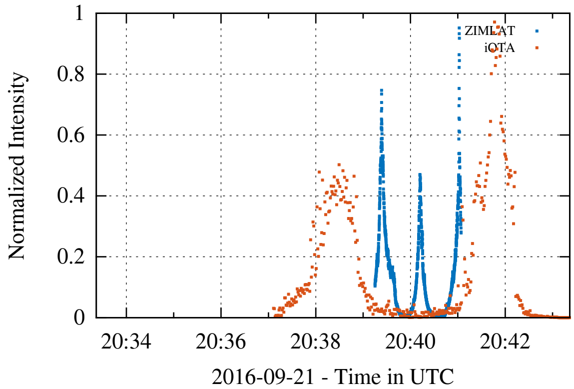

Figure 16. ENVISAT simulated light curve, second passage

In a first step, due to the high processing time consumption, only the following perturbation sources have been included in the simulation:

- Gravitational force and torque for the orbit and attitude motion prediction
- 3rd body perturbation for the orbit prediction
- Eddy currents for the attitude motion prediction

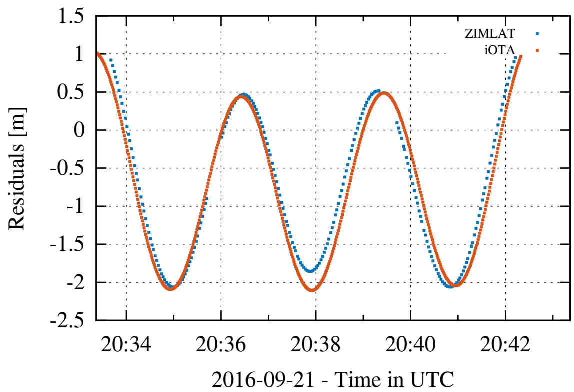

Figure 17. ENVISAT simulated SLR residuals, second passage

Solar radiation pressure and atmospheric drag have been excluded to decrease the processing time. The obtained results have been compared qualitatively, see Fig. 23, with the values determined by AIUB from SLR residuals measurements acquired for ENVISAT by ZIMLAT telescope during the years 2013–2014. The simulated angular velocity decreases over time in good agreement with

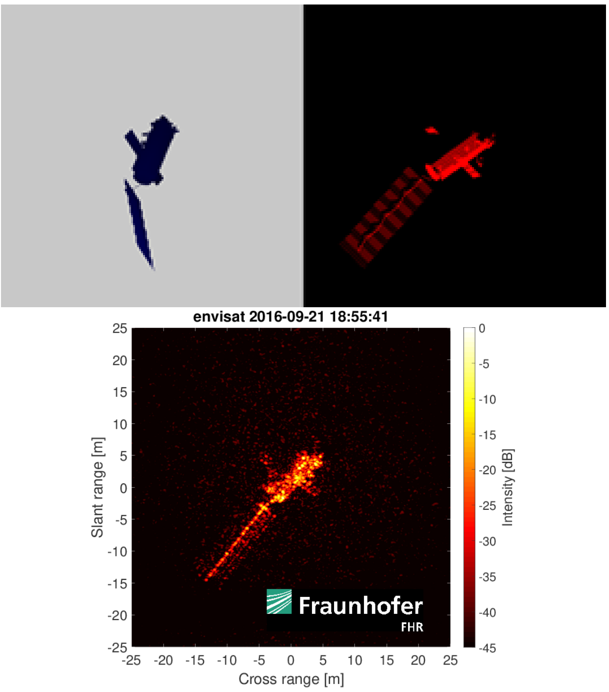

Figure 18. ENVISAT simulated optical view (top left) and ISAR (top right), real ISAR (bottom), first passage, part 1

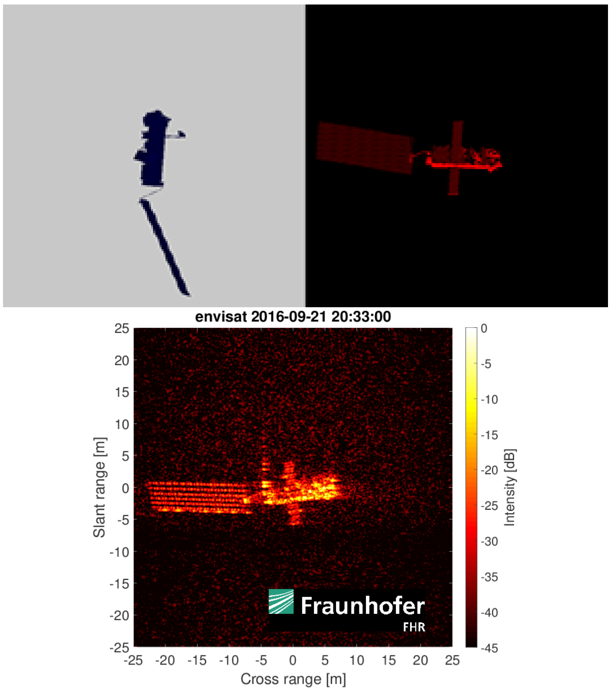

Figure 20. ENVISAT simulated optical view (top left) and ISAR (top right), real ISAR (bottom), second passage, part 1

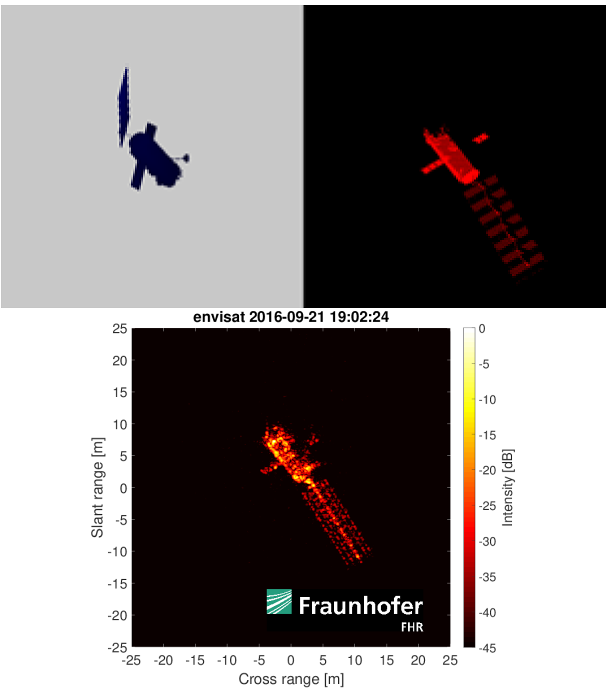

Figure 19. ENVISAT simulated optical view (top left) and ISAR (top right), real ISAR (bottom), first passage, part 2

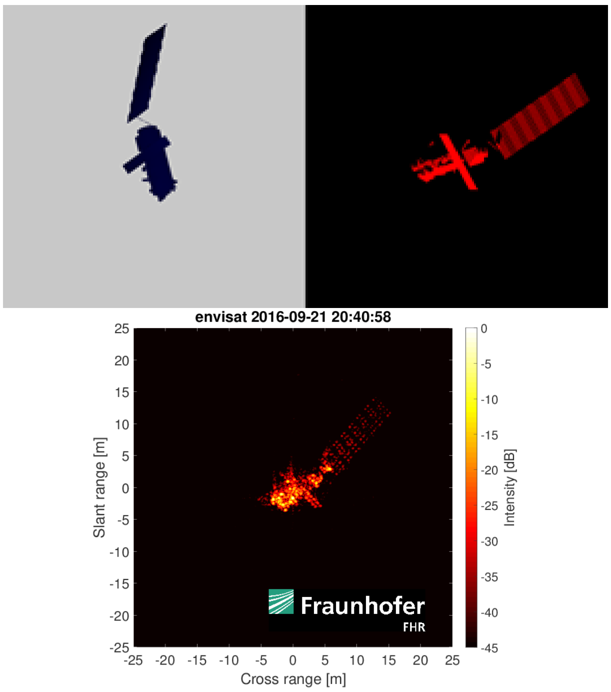

Figure 21. ENVISAT simulated optical view (top left) and ISAR (top right), real ISAR (bottom), second passage, part 2

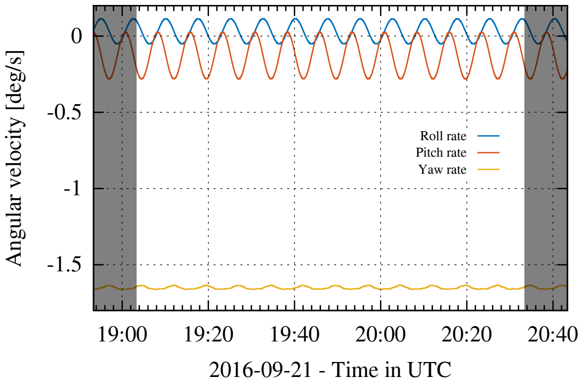

Figure 22. ENVISAT simulated angular velocities (passages marked in gray)

the real measurements. However, the SLR measurements show some indication for periodic angular velocities increases which could not be reproduced with ιOTA if solar radiation pressure is excluded.

After including all external forces and torques in the simulation, i.e. aerodynamics, eddy current damping, gravity and solar radiation pressure, the long-term evolution of the ENVISAT angular velocity shows a zig-zag pattern indicating that there are phases of angular momentum increase and phases of angular momentum decrease following each other periodically, as shown in Fig. 24. This pattern is driven by the yaw rate mostly, because of the initial state assumption of roll and pitch rate being zero.

The angular acceleration caused by solar radiation pressure (see Fig. 25) reveals that this periodic behavior is caused by solar radiation pressure on the solar array of ENVISAT. When the solar array is illuminated in spin direction, solar radiation pressure increases the spin rate of ENVISAT, adding angular momentum. Through precession and nutation, the spin axis changes over time, transferring components of the spin to the roll and pitch axes (see drops in yaw rate in Fig. 24). Periodically, the orientation of the solar array w.r.t. the illumination by solar radiation is flipping. Thus, after adding angular momentum for one period, angular acceleration from solar radiation pressure is directed in counter-spin direction for the following period, decelerating the rotation.

7. SUMMARY, CONCLUSIONS, OUTLOOK

This paper has described the In-Orbit Tumbling Analysis tool (ιOTA), a software prototype developed by HTG for ESA, and how the software has been validated in the context of a collaborative measurement campaign, involving multiple European research partners.

The simulated SLR residuals and ISAR images for ENVISAT show a very good agreement with the real observations. The simulation of light curves for complex ob-

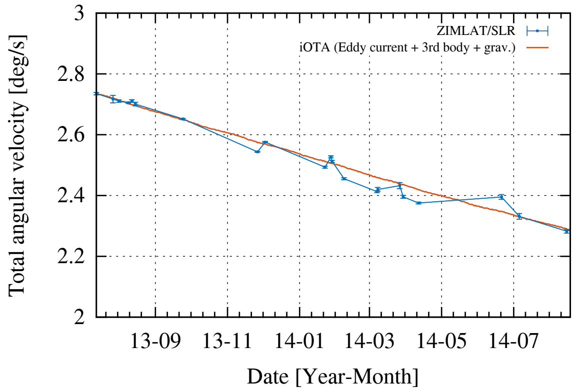

Figure 23. ENVISAT long-term angular velocity observation/simulation

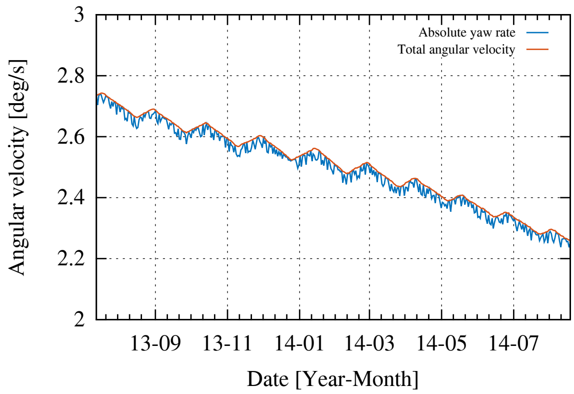

Figure 24. ENVISAT long-term angular velocity simulation

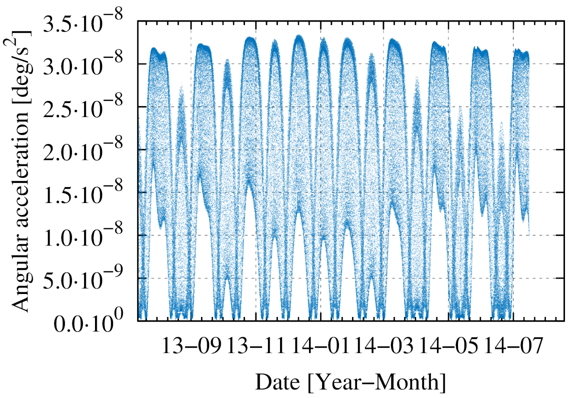

Figure 25. ENVISAT long-term solar radiation perturbations

jects like ENVISAT has turned out to be difficult, at least if a very simple light reflection model is used. Therefore, future versions of ιOTA should include more detailed, non-unique light reflection models.

Furthermore, future development of ιOTA should address computation time improvements (e.g. by using GPU computing or pre-computed aerodynamic databases) and the implementation of an optimization module for automated identification of the best match between observations and simulations.

ACKNOWLEDGEMENTS

The work presented in this paper was funded under ESA Contract No. 4000112447/14/D/SR.

REFERENCES

1. Kanzler R., et al., (2015). *Space debris attitude simulation - ιOTA (In-Orbit Tumbling Analysis)*, Presented at The Advanced Maui Optical and Space Surveillance Technologies (AMOS) Conference 2015, Maui, Hawaii, USA
2. Šilha J., et al., (2016). *Comparison of ENVISAT's attitude simulation and real optical and SLR observations in order to refine the satellite attitude model*, Presented at The Advanced Maui Optical and Space Surveillance Technologies (AMOS) Conference 2016, Maui, Hawaii, USA
3. Picone J.M., et al., (2002). *NRLMSISE-00 empirical model of the atmosphere: Statistical comparisons and scientific issues*, J. Geophys. Res., 107 (A12), 1468, doi: 10.1029/2002JA009430
4. Lemoine F.G., et al., (1998). *The Development of the Joint NASA GSFC and NIMA Geopotential Model EGM96*, NASA/TP-1998-206861
5. Pavlis N.K., et al., (2012). *The development and evaluation of the Earth Gravitational Model 2008 (EGM2008)*, J. Geophys. Res., 117, B04406, doi: 10.1029/2011JB008916
6. Vallado D.A., (2013). *Fundamentals of Astrodynamics and Applications*, 4th Edition, Microcosm Press
7. NASA JPL Solar system dynamics, HORIZON system, http://ssd.jpl.nasa.gov/?horizons
8. Chulliat A., et al., (2014). *The US/UK World Magnetic Model for 2015-2020*, NOAA National Geophysical Data Center, Boulder, CO, doi: 10.7289/V5TH8JNW
9. Praly N., et al., (2012). *Study on the eddy current damping of the spin dynamics of space debris from Ariane launcher upper stages*, Acta Astronautica, Vol. 76, p. 145-153
10. Ortiz Gómez N., Walker S., (2015). *Earth's gravity gradient and eddy currents effects on the rotational dynamics of space debris objects: Envisat case study*, Advances in Space Research, Vol. 56, Issue 3, p. 494-508
11. Lips T., et al., (2007). *Re-entry Risk Assessment for Launchers – Development of the new SCARAB 3.1L*, Proceedings of the Second IAASS Conference, SP-645, ESA Communication Production Office, ESTEC, Noordwijk, The Netherlands